

Supporting Information:

Cubic Polyoxometalate-Organic Molecular Cage

Shou-Tian Zheng,[†] Jie Zhang,[†] Xin-Xiong Li,[†] Wei-Hui Fang,[†] and Guo-Yu Yang*,^{†,‡}

[†] State Key Laboratory of Structural Chemistry, Fujian Institute of Research on the Structure of Matter, Chinese Academy of Sciences, Fuzhou, Fujian 350002 (China); [‡] MOE Key Laboratory of Cluster Science, Department of Chemistry, Beijing Institute of Technology, Beijing 100081 (China).

This file includes:

Section S1. Experimental Section	S2
Section S2. Additional Structural figures	S3
Section S3. Additional TGA, magnetic figures, IR, PXRD, and EDS	S4-S8

Section S1. Experimental Section

Synthesis of 1: $\text{Na}_9[A\text{-}\alpha\text{-PW}_9\text{O}_{34}]\cdot\text{nH}_2\text{O}$ (**PW₉**) were prepared by literature method (*Inorganic Syntheses*, John Wiley & Sons: New York, **1990**, vol. 27, p 85). A sample of 0.30 g **PW₉** was stirred in 10 ml of a 0.5 M sodium acetate buffer (pH 4.8), and then 0.40 g Tris was added. After stirring for 5 min, 0.80 g $\text{NiCl}_2\cdot 6\text{H}_2\text{O}$ was added in the above solution with continuous stirring. Further, to this solution 0.30 ml en (en = ethylenediamine) and 0.25 g sodium 1,3,5-benzene-tricarboxylate are in turn added and stirred for 45 min. The resulting solution was sealed in a 35 mL stainless steel reactor with a Teflon liner and heated at 160 °C for 25 hours, and then cooled to room temperature. Accordingly, green block crystals of **1** were obtained (28.2 % yield based on Ni). Anal. Calcd (Found %) for $\text{C}_{236}\text{H}_{616}\text{N}_{104}\text{Ni}_{54}\text{O}_{434}\text{P}_8\text{W}_{72}$ **1**: C, 9.93 (10.32); H, 2.18 (2.73); N, 5.11 (5.01). According to the EA and TGA, there are twelve en molecules and fifty-four water molecules located in the structure, but these couldn't be unambiguously located by X-ray analysis.

Single-crystal structure analysis: Crystal data of **1**: $M_r = 28511.63$, Hexagonal, $R\text{-}3$, $a = 33.915(5)$, $c = 59.795(8)$ Å, $V = 59564(15)$ Å³, $Z = 3$, $\rho = 2.385$ g cm⁻³, $\mu = 11.728$ mm⁻¹, $F(000) = 39576$, GOF = 1.072, A total of 146332 reflections were collected in the range of $2.29^\circ \leq \theta \leq 27.48^\circ$, 28964 of which were unique ($R_{\text{int}} = 0.1221$). $R_1(wR_2) = 0.0959(0.2131)$ for 1332 parameters and 22630 reflections ($I > 2\sigma(I)$). CCDC-759738. X-ray diffraction data were collected on a Mercury-CCD diffractometer with graphite-monochromated MoK α ($\lambda = 0.71073$ Å) at room temperature. The program SADABS was used for the absorption correction. The structures were solved by the direct method and refined on F^2 by full-matrix least-squares methods using the SHELX97 program package.

Others: IR spectra were recorded on a Nicolet AVATAR 370 FT-IR infrared spectrophotometer. Thermal analyses were performed in a dynamic oxygen atmosphere with a heating rate of 10 °C/min, using a METTLER TGA/SDTA851° thermal analyzer. Powder XRD patterns were obtained using a Philips X'Pert-MPD diffractometer with CuK α radiation ($\lambda = 1.54056$ Å). Variable temperature susceptibility measurements were carried out in the temperature range 2-300 K at a magnetic field of 0.5T on polycrystalline samples with a Quantum Design QD PPMS-9T magnetometer. The experimental susceptibilities were corrected for the Pascal's constants. Elemental analyses of C, H and N were carried out with a Vario EL III elemental analyzer. Energy-dispersive X-ray spectroscopy (EDS) measurement was performed on a JSM-6700F scanning electron microscope.

Section S2. Additional structural figures

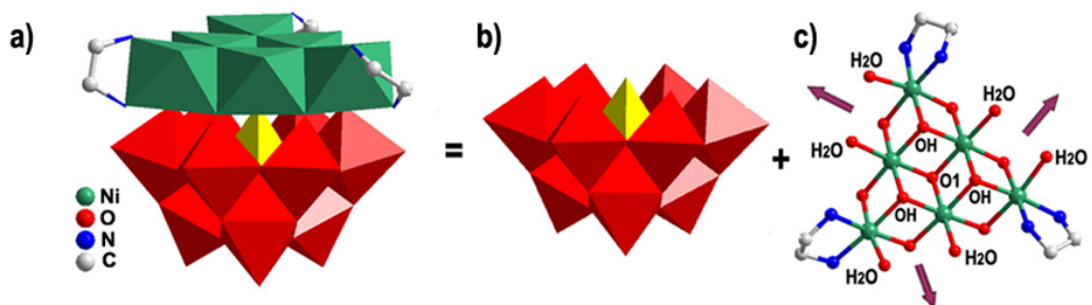


Figure S1. a) Structure of $[Ni_6(\mu_3-OH)_3(H_2O)_6(en)_3(B-\alpha-PW_9O_{34})]$ (Ni_6PW_9). b) and c) Structures of $B-\alpha-[PW_9O_{34}]^9$ and inorganic-organic hybrid Ni_6 cluster, respectively. WO₆, red; NiO₆ or NiO₄N₂, green; PO₄, yellow.

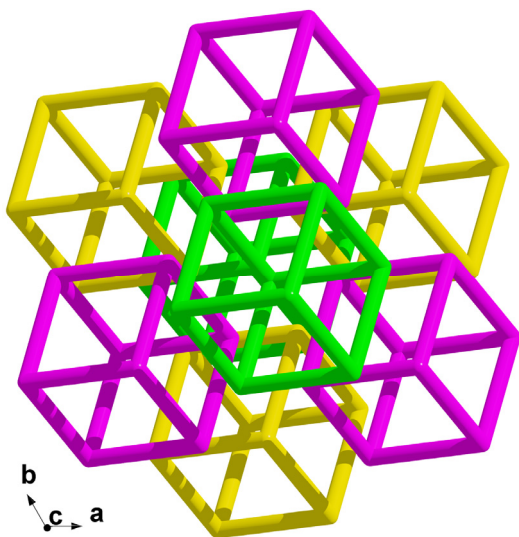


Figure S2. View of the 3D hexagonal close-packed structure of **1** along the *c*-axis. Tris-grafted Ni_6PW_9 and the 1,3,5-BTCs are simplified as 3-connected nodes and linear bars respectively.

Section S3. Additional PXRD, TGA, magnetic figures, IR, and EDS

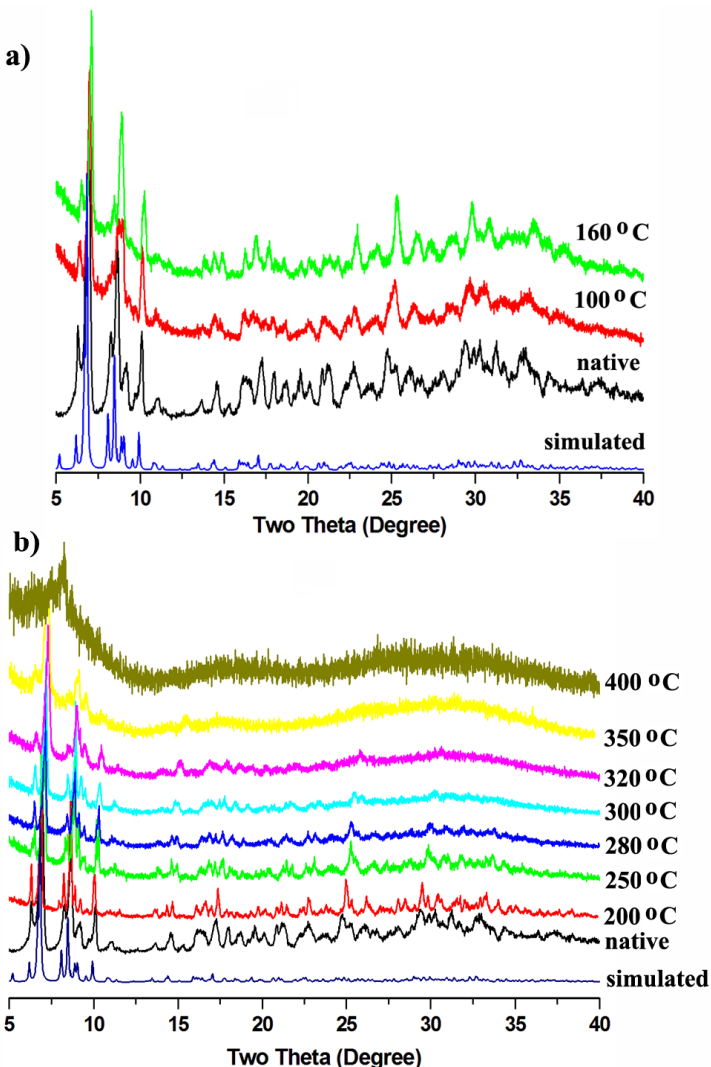


Figure S3. a) Hydrothermal stability of the as-synthesized sample **1**. b) Thermodiffractograms of the as-synthesized sample **1**.

Except the fascinating structural features, **1** also represents high hydrothermal stability and thermal stability. Powder X-ray diffraction (PXRD) patterns indicate **1** is stable in boiling water for 24 hours and doesn't collapse even under 160 °C hydrothermal conditions for 24 hours (Figure S3a), which is not common for metal-organic framework materials. Further, thermal gravimetric analysis of **1** shows that the removal of crystallographic water and isolated en molecules occurs in the temperature range of 40~150 °C and no further weight loss up to 300 °C (Figure S4). PXRD patterns confirm that the desolvated sample retain its crystallinity up to about 350 °C (Figure S3b).

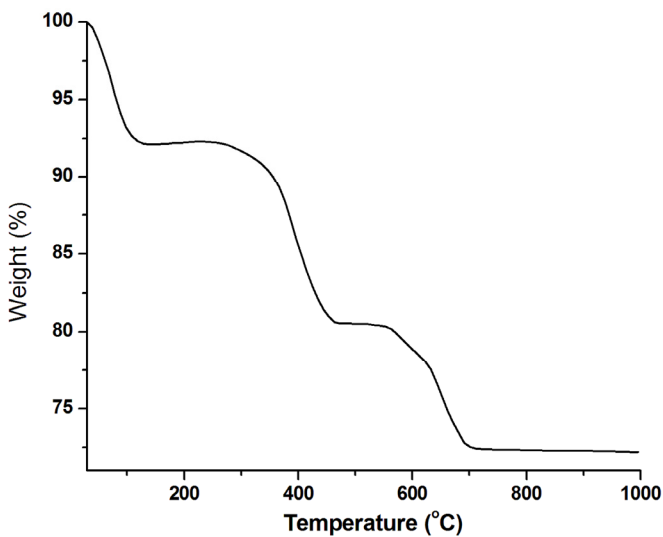


Figure S4. TGA curves of **1**.

The thermogravimetric analysis carried out in a flow of air at a heating rate of 10 °C/min for **1** indicates that the weight loss shows three major steps of weight losses. The first weight loss corresponds to the removal of lattice water molecules and isolated en molecules at relatively lower temperature (45 ~ 150 °C). The remainder two stages (in the ranges 300 ~ 450°C and 550 ~ 700 °C) are mainly attributed to the loss of the organic ligands and the sublimation of P₂O₅. Assuming that the residue corresponds to WO₃ and NiO, the observed weight loss (27.7%) is in good agreement with the calculated value (27.3%).

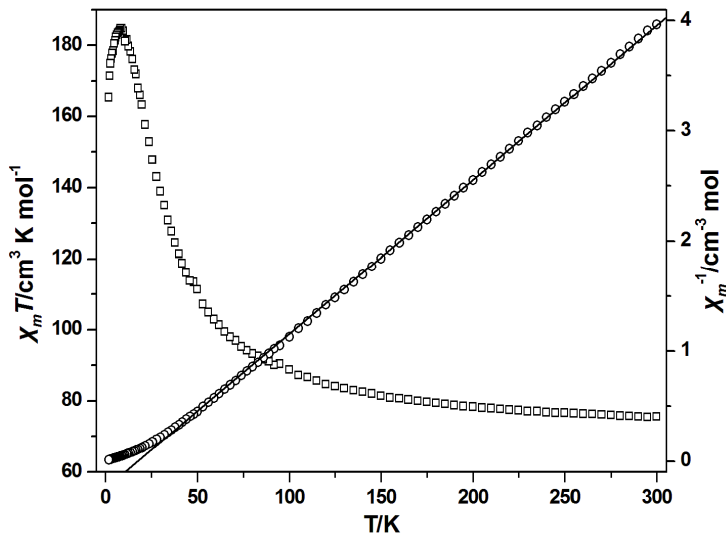


Figure S5. Temperature dependence of $\chi_m T$ (□) and χ_m^{-1} (○) for **1**.

Various temperature magnetic susceptibilities for **1** was measured in the temperature range 2-300 K with an applied magnetic field of 1 kOe (Figure S5). The experimental $\chi_m T$ value of **1** at 300 K is 72.64 cm³·mol⁻¹·K,

which is expected for 54 uncoupled high-spin Ni^{2+} ions with $S = 1$ and $g > 2.0$. Upon cooling, the $\chi_m T$ values of **1** increase to a maximum of $184.78 \text{ cm}^3 \cdot \text{mol}^{-1} \cdot \text{K}$ at 9.02 K corresponding to the value of $176 \text{ cm}^3 \text{ mol}^{-1} \text{ K}$ expected for six isolated $S = 1$ Ni ions and eight $S = 6$ (Ni_6) ground states subunits with $g = 2.0$, then decrease sharply to reach $165.34 \text{ cm}^3 \cdot \text{mol}^{-1} \cdot \text{K}$ at 2.0 K , where the sudden decrease might be mainly attributed to the presence of zero-field splitting and inter-cluster magnetic interactions. The above behaviors suggest that there exist overall ferromagnetic interactions between the Ni^{2+} ions. The temperature dependence of the reciprocal susceptibilities ($1/\chi_m$) obeys the Curie-Weiss law above 50 K with positive $\theta = 17.7 \text{ K}$, which support the presence of overall ferromagnetic coupling between the Ni^{2+} ions. The Curie constants $C = 71.3 \text{ cm}^3 \text{ mol}^{-1} \text{ K}$ is reasonable for 54 Ni^{2+} ions per formula, respectively. Ac magnetic susceptibilities of **1** with frequencies between 111 and 3511 Hz were measured under $H_{\text{ac}}=3 \text{ Oe}$ (Figures S4), but no frequency dependence is observed. Isothermal magnetizations $M(H)$ at 2 K show magnetization increases from 0 to 70 kOe, reaching 113.8 at 70 kOe (Figure S5), which is in accordance with the saturation values $M_S = 108$ for 54 Ni^{2+} ions.

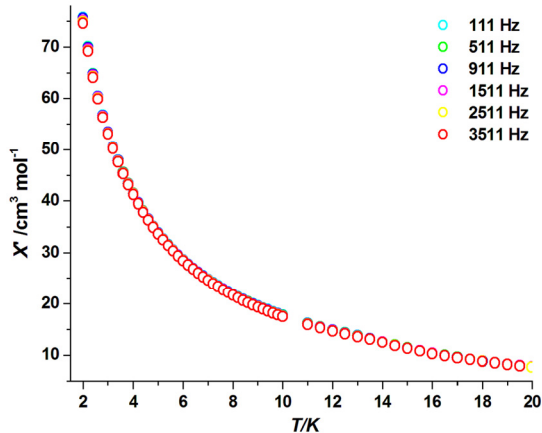


Figure S6. Frequency-dependent behavior of χ' for **1** in zero static field.

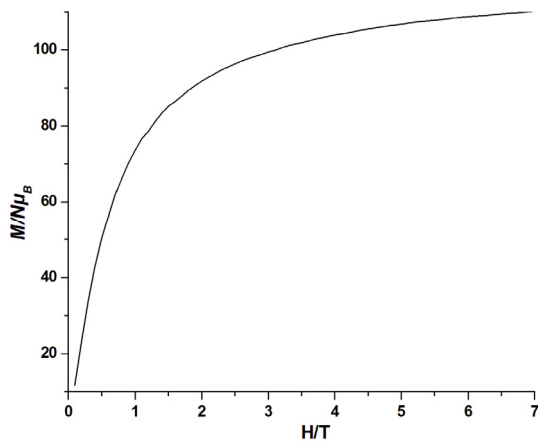


Figure S7. Magnetization measurement, in the reduced form of $M/N\mu_B$, in the field range 0 - 7 T at 2 K of **1**.

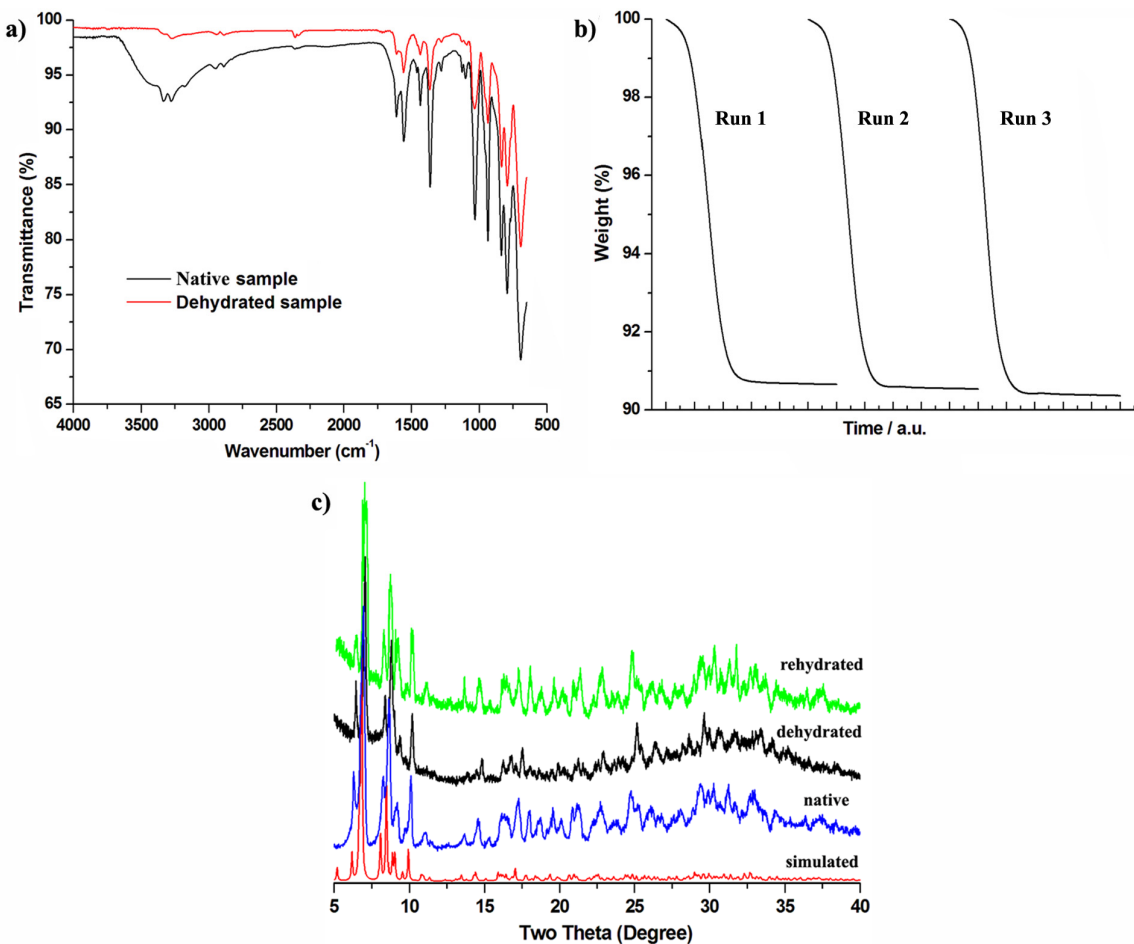


Figure S8. a) IR spectra of **1** before and after heated at 200 °C for one hour. b) TGA water desorption of **1** showing three consecutive runs. c) PXRD patterns of **1** as simulated from single crystal XRD, native sample, after dehydration and after rehydration (room temperatures).

Powder X-ray diffraction (PXRD) patterns indicate **1** is stable in boiling water for 24 hours and doesn't collapse even under 160 °C hydrothermal conditions for 24 hours (Figure S3a). Additionally, thermal gravimetric analysis (TGA) of **1** shows that the removal of crystallographic water and isolated en molecules occurs in the temperature range of 40~150 °C and no further weight loss up to 300 °C (Figure S4). PXRD patterns further confirm that the desolvated sample retain its crystallinity up to about 350 °C (Figure S3b). Compared with the sample before heating (Figure S8a), the absence of the broad and strong $\nu(\text{OH})$ band at 3340 cm^{-1} of heated sample indicates the crystallographic water in **1** can be removed at 200 °C. These results show **1** has high thermal and hydrothermal stability. Thus, thermogravimetric water sorption experiments were undertaken to study the reversible inclusion of crystallographic water of **1**. Firstly, a copy of dehydrated sample of **1** was prepared by heating at 200 °C for one hour to a constant weight. And then, after exposing the sample to ambient atmosphere for 24 h, TGA showed that the water can be re-adsorbed. It has shown that the sample desorbs ~ 9.2 % of crystal water, and within 24 h can re-adsorb a similar amount of water from the atmosphere. Each of this procedure was repeated several times to demonstrate the reversibility of the process (Figure S8b).

Further, the stability of the sample was investigated by PXRD which indicated that the sample retained their crystallinity after several desorption and re-adsorption cycles for solvent water (Figure S8c).

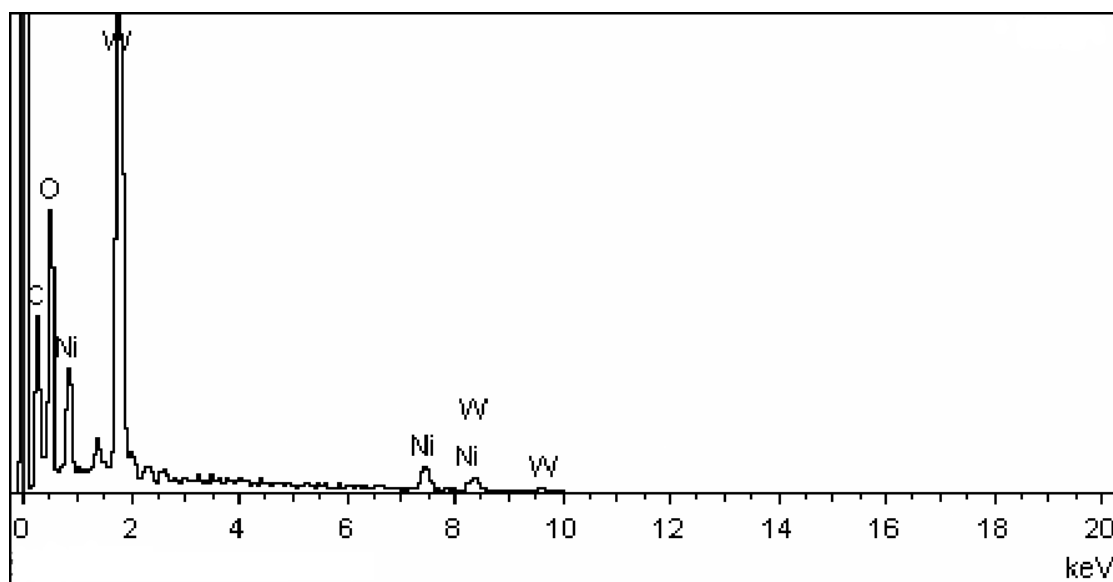


Figure S9. Energy-dispersive X-ray spectroscopy of **1**, showing there is no sodium in the structure.